2nd IFAC Workshop on Automatic Control in Offshore Oil and Gas Production,
May 27-29, 2015, Florianópolis, Brazil

Results of Real-Time Production Optimization of a maturing North Sea Gas Asset with Production Constraints

R.J.P. van der Linden*, J.W. Marck*, J.P. de Boer*

**TNO Heat Transfer and Fluid Dynamics, Delft, P.O. box 155, 2600 AD The Netherlands (Tel: +31 888665647, ruud.vanderlinden@tno.nl).*

Abstract: Operating maturing assets poses increasingly complex challenges to operators. Meeting hourly or daily production targets becomes more difficult when wells are more often shut in for e.g. water washes (against salt deposition) or solvent jobs (at asphaltenes deposition). Declining reservoir pressure in turn results in less margin to compensate lost production while topside facilities can put constraints when production GOR and watercut increase at late production life. In a joint industry project of Wintershall, GdF, EBN, Siemens and TNO the applicability of real-time optimization is explored. The problem description, system architecture and initial optimizer results were presented in Linden (2013). This paper presents results of the optimization project and looks ahead to further field realization. The goal of this paper is to demonstrate that production of a mature North Sea gas asset can be optimized taking into account realistic constraints. All wells at this gas asset are intermittently shut in for water washes while daily nominations must be met. It will be shown that the optimization algorithm obeys the constraints and is fast enough for real-time application and thereby ready for field implementation.

Keywords: Real-time, Optimization problems, Model reduction, Prediction methods, Gas turbines.

1. INTRODUCTION AND PROBLEM DESCRIPTION

The asset considered in this study consists of a satellite platform (3 wells) connected to a main platform (5 wells). The satellite platform is connected to the main platform at which two separator trains in operation, and two compressor trains. Individual wells can be switched between separator trains through manifolds and compressor selection is possible downstream of the joint separator gas outlet. For a schematic layout of the 8-well system, see Figure 1.

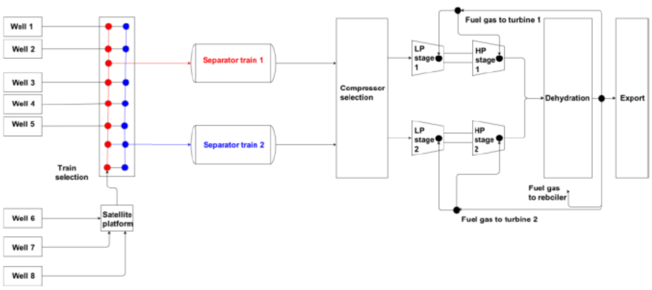

Fig. 1. Schematic asset layout with wells (left), separator trains (middle) and compressor trains (right).

Production of this asset is characterized by:

- Fast decline of well pressure due to salt precipitation in the well/near-wellbore. This results in frequent shut-in of wells and fresh water washing operations. For the least performing wells the production/wash cycle spans a few days;
- Dynamic behavior of the wellhead pressure after a well starts producing, due to pressure buildup in the near-wellbore;
- Topside compression constraints (depending on number of wells producing);
- Rerouting of wells to maximize production and cope with well start-up of wells prone to liquid loading;
- (Slow) degradation of compressor performance due to salt;
- Slow decline of reservoir pressure.

The optimizer qualifies for field application if the optimization algorithm proves able to cope with all of the above dynamics and constraints. The optimization algorithm is applied to optimization objectives, representing operational considerations. The two objectives are:

1. Minimize compressor fuel gas consumption while delivering a required hourly production target (Q_{SP}) in a steady production state:
2. Minimize overall operational cost while delivering a daily production target. Operational cost consist of fuel cost and penalties for under/overproduction (if inevitable):

The corresponding objective functions are respectively:

$$\min J = Q_{fuel}(k) + W\big(Q(k) - Q_{sp}(k)\big)^2 \qquad (1)$$

and

$$\min J =$$

$$\sum_{k_0}^{24/\Delta t} Q_{fuel}(k) + W\left[\left(IQ_{sp} - IQ(k_o)\right) - \sum_{k_0}^{24/\Delta t} Q(k)\right]^2 \quad (2)$$

Note that any term can be added to such objective function, as long as the required output (e.g. instantaneous compressor rpm, or cumulative water production) is calculated by the network model. The network model properties will be discussed in the section 'Method'.

The actual asset dynamics as they appear in the field were discussed above. The available actions ("manipulated variables") in this optimization problem are:

- Compressor turbine rpm
- Choke setting of a limited number of wells
- Compressor train recycle valve

Optimal routing of wells (e.g. matching total rates to compressor trains, or matching high/low pressure wells) and wash-cycle time optimization are not included in the current optimization problem. Practical constraints arise from gas well liquid loading minimum production rates, see Belfroid et al (2008) and Veeken (2010). Constraints in terms of maximal flow rates can be set to limit erosion.

2. METHOD

A full physics-based network model is setup to predict asset behavior with maximum accuracy against minimal calculation time and minimal fitting effort. Each well consists of a reservoir, well- and choke model. At the topside manifold well streams meet, depending on separator and compressor routing). The asset model ends downstream of the compressor train, at export facilities. The asset network model is broken down into the components:

- Reservoir model, calculating the reservoir pressure P_{RES} as function of production flow Q;
- Dynamic wellbore, adds a dynamic term to P_{RES} to capture well dynamics around shut-in;
- Well model, calculates the tubing head pressure *THP* from the reservoir pressure and production flow Q;
- Salt model, additional pressure drop for the well model based on the cumulative gas production since last water wash;
- Choke model, calculates the choke pressure drop corresponding to a gas flow rate using classic single-phase orifice relations;
- Compressor model, calculates the required compressor rpm (and through efficiency, the fuel) to achieve a certain suction pressure using Odom (2009) and *Data collection and analysis of the combined heat and power system at Eastern Maine Medical Center,* (2008)

The pressure drop in the topside piping between the chokes and compressor inlet is set to the constant value of 1.0 bar, based on field measurements.
For the individual components literature models are available to relate the observed pressure drop to estimated gas flow rate. This is required for the optimizer to determine which change in manipulated variable (choke, compressor rpm, …) is necessary to find the optimal operational strategy.

Since no bottom hole pressure measurements are available, the reservoir-wellbore are combined into a single, total pressure drop. This also includes a data-driven pressure drop representing the salt deposition in the near-wellbore. For each well, the decline due to salt precipitation is a function of cumulative gas production since the last water wash. Parameters for this are fitted to well test intervals when flow measurements are available. Figure 2 shows the relations between the models and indicates which quantities are available from field measurements.

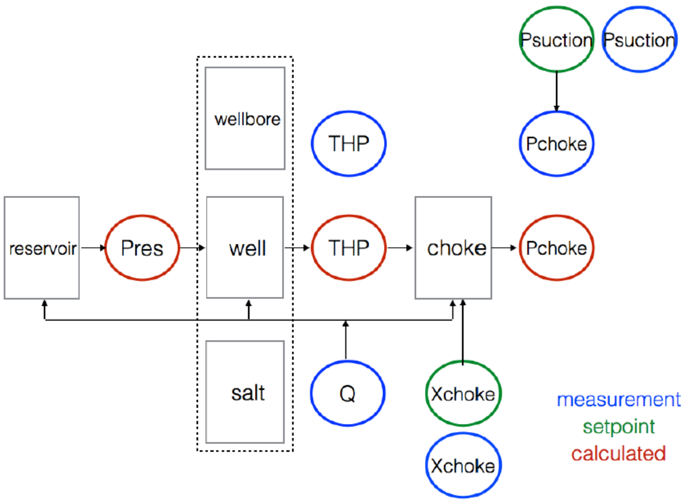

Fig. 2. Reservoir-well-choke models and key variables.

The reservoir consists of a two-tank model, to account for pressure build-up in the near-wellbore. A Cullender-Smith model is used to relate flow and pressure drop over the wellbore (Chaudhry, 2003). The models are validated according to Figure 4 and the overall flow estimation (using the combined reservoir-well-choke models) is compared against intervals during which flow measurements are available. The available measurements are:

- Q: wet gas flow sensor (hourly, during well test intervals only)
- *THP*: tubing head pressure (continuously)
- X_{CHOKE}: choke position/opening (continuously)
- $P_{SUCTION}$: compressor suction pressure

With flow rate measurements being available hourly, the calculations for the asset optimization are performed hourly as well, as will be presented below.

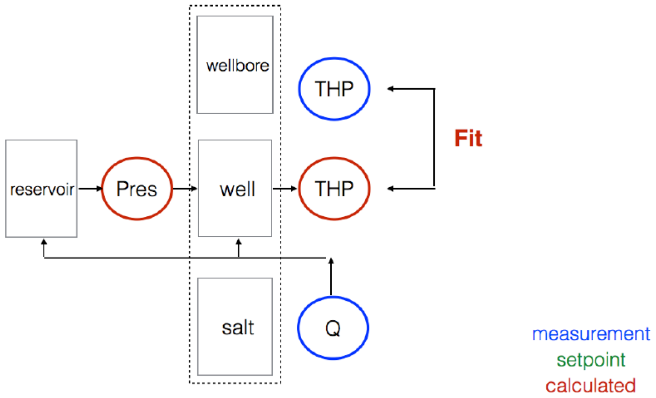

Fig. 3. Configuration of the resrvoir-well model fit: tubing head pressure (*THP*) is calculated from measured flow (*Q*) and compared against measured *THP*.

In contrast to the reservoir and salt models, the choke model is time invariant and was therefore fitted to all measurement values during 6 months of field data of *THP* and P_{CHOKE}, and X_{CHOKE}. Note that P_{CHOKE} is equal to the compressor inlet pressure (apart from 1 bar pressure drop in topside piping), therefore indicated as measurement in Figure 4.

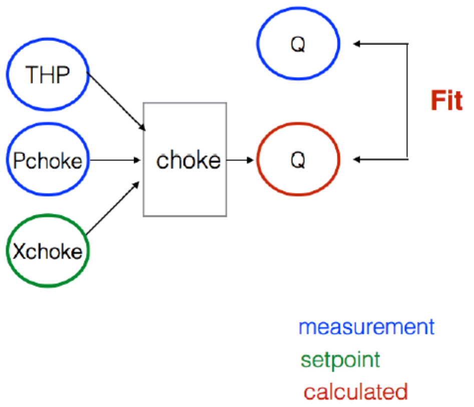

Fig. 4. Configuration for choke model fit: choke flow *Q* is calculated from measured pressure P_{CHOKE}, set choke opening X_{CHOKE} and measured tubing head pressure *THP* and compared against measured flow *Q*.

In the fitting of the choke model, parameters *a* and *b* were used to describe the relation between choke position X_{CHOKE} and choke coefficient of discharge opening C_D:

$$C_d = a\left(1 - \exp(-bX_{CHOKE})\right) \tag{3}$$

For the majority of wells, this flow rate estimation is within 10% of actual gas flow rate measurements. Deviations were present at small choke sizes, which are underrepresented in the fitting of choke parameters over the 6 months of $THP/P_{CHOKE}/X_{CHOKE}$ data.

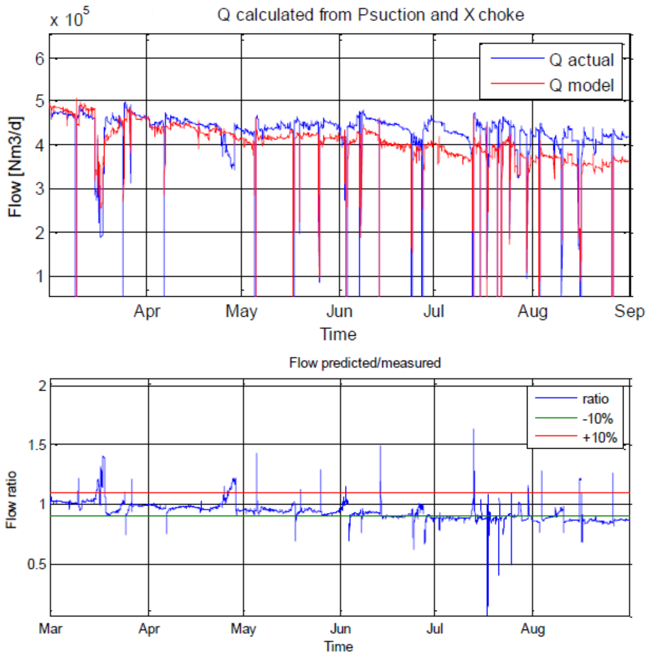

Figure 1. Comparison of predicted (red, top) and measured (blue, top) gas flow rates. Bottom panel shows ratio of predicted and measured flow rates, with +10% (red) and -10% (green) error bounds.

As can be observed in Figure 1 (bottom panel), the predicted flow drifts away from the actual flow rate. The model deviates more than 10% when predicting more than ~3 months ahead. A slowly-correcting median filter is applied over the last *N* measurements to compensate for this drifting. Median filters are relatively insensitive to outliers (spikes) as appear in the field data. Based on the last *N* samples, an offset is estimated and compensated for at every new measurement:

$$c(k) = \\ median\left(y_{measured}(k-N+1:k) - y_{predicted}(k-N+1:k)\right) \tag{4}$$

The resulting corrected and uncorrected flow rate estimation are shown in Figure 7 for one of the asset's wells. As can be seen, the drift is completely compensated for when taking a window size of 14 days.

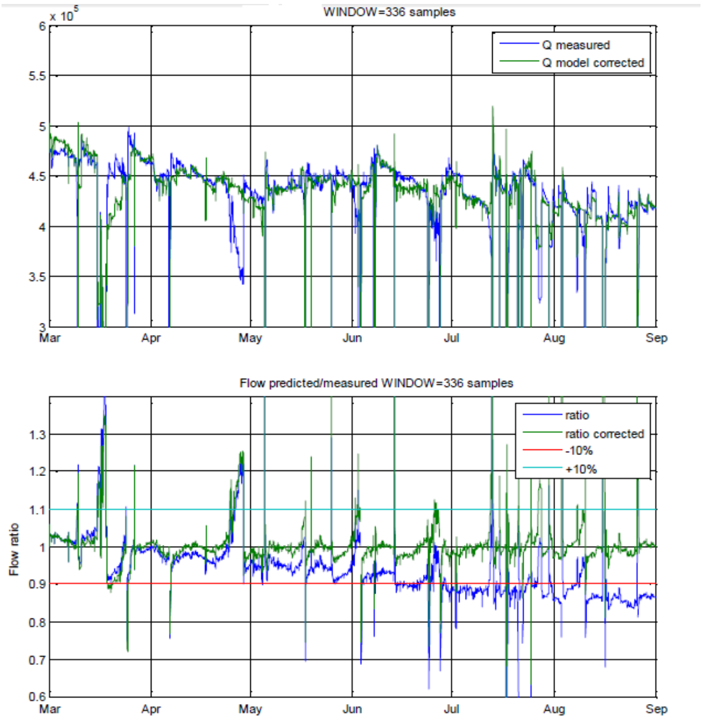

Fig. 7. Corrected (green) and uncorrected (blue) flow prediction ratio (predicted/measured) with a median filter window size of 14 days (336 samples). Red and light blue indicate -10% and +10% error bounds respectively.

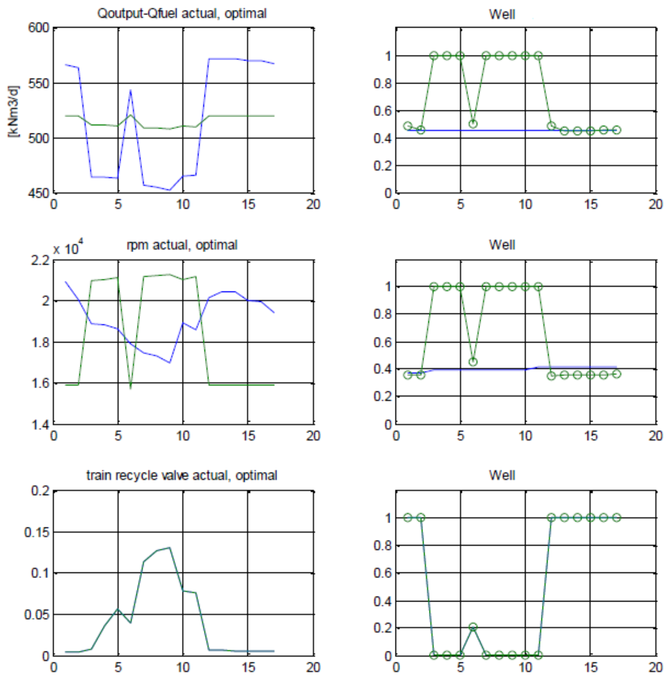

Fig. 8. Actual settings as applied in field (blue) and optimal strategy (green) for the 17-hour interval. Choke of well C (shut in) is not included in this optimization. Horizontal axis represents time in hours.

Based on the verified performance of the overall reservoir-well-choke models to estimate gas flow rates, the actual optimization problem can now be initiated.

3. RESULTS

The performance of the optimizer has been analyzed against two intervals of actual production data. Interval 1 is optimized for the objective function as in (1), while Interval 2 was optimized for objective function as described in (2).

Interval 1 consists of a 17-hour time window, capturing a shut-in of well E (bottom right, Figure 8) for a water wash to dissolve precipitated salt. Despite the shut-in, the daily gas supply requirement must be met and compressor fuel consumption minimized.

The left panels of Figure 8 show that the optimal compressor rpm and fuel consumption are quite different from the actual applied strategy. The train recycle valve is not used (Below 10% opening the recycle valve is closed) as seen in the bottom left panel in Figure 8) in this optimization since surge can be avoided by controlling the chokes of Well A and C. Compressor fuel reduction is not reduced significantly since both the decrease in compressor rpm is accompanied by a drop in compressor efficiency.

Interval 2 covers 24 hours of operations covering a shut-in of well A, during which the daily production requirements of the asset must still be met.

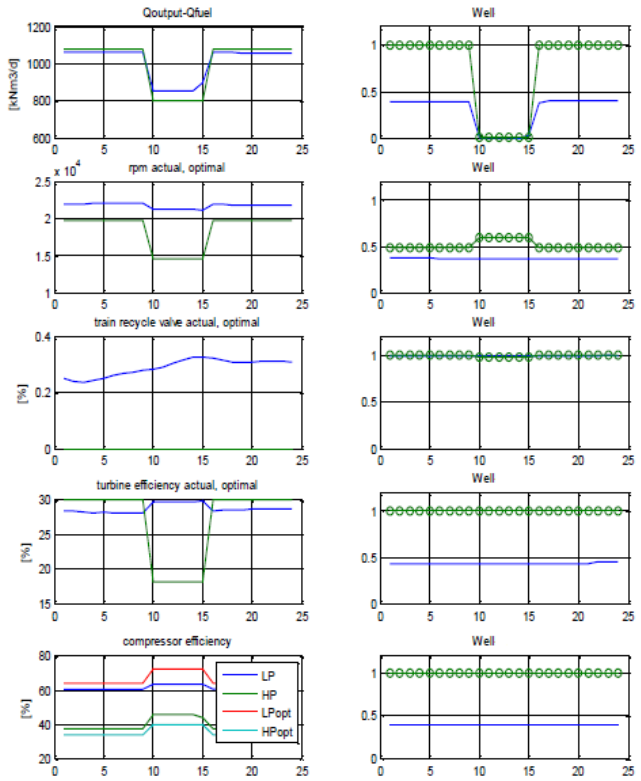

Figure 2. Actual (blue) and optimal (green) strategies during Interval 2, for platform production (left, upper), compressor settings (left, second panel from top), train recycle valve (left, middle) and choke settings for wells A-E. Resulting compressor and turbine efficiency shown in left lower figures. Horizontal axis represents time in hours.

The optimization decreases the flow rate during the shut in interval of well A and compensates production loss during shut-in when all wells are operating. This strategy reduces the required average compressor power during the optimized 24-hour interval from 4.4 MW to 3.5 MW by applying the optimal strategy. The compressor efficiency reduction accompanied with the reduced compressor flow is much less than during Interval A, yielding a fuel consumption reduction of 18%.

6. CONCLUSIONS

Both example intervals showed that optimization of asset production was achieved according to the posed constraints. Due to the different response of each well to topside pressure variations, optimizing production is not straightforward. Accurate representation of asset performance was achieved through component-wise physics-based models, allowing for a prediction window up to 6 months. The optimization algorithm always converged to an optimal solution and random checks showed it actually converged to global maxima.

The optimization calculation time varied from less than 1 minute to maximum 20 minutes. With flow rate measurements being available hourly, the algorithm can be applied 'as-is' to this North Sea asset for real-time applications. It is expected that the calculation time can be reduced significantly.

The presented case shows that real-time optimization technology is ready to be implemented as integrated method for asset performance evaluation under real-life conditions. Additionally, it can assist in immediate decision support, e.g. at unplanned well shut-ins.

Similar work is ongoing for multiphase flow production modelling, where achieving accurate flow rate estimations is more challenging.

NOMENCLATURE

J	Objective function
Q	Gas flow rate
Q_{SP}	Set point gas flow rate
IQ_{SP}	Daily gas nomination set point
W	Weighting parameter
a	Choke model fit parameter
b	Choke model fit parameter
c	Median-filter correction
C_D	Choke discharge coefficient
k	Time index

REFERENCES

Belfroid, S.P.C et al (2008), Analyzing the effect of well parameters on critical velocity, European Gas Well Deliquification Conference.

Chaudhry, A.U. (2003) *Gas Well Testing Handbook*, Gulf Professional Publishing. Elsevier.

Data collection and analysis of the combined heat and power system at Eastern Maine Medical Center, (2008) CDH Energy Corp, Available at: www.energy.gov [Accessed: 3 November 2014].

Odom, F and Muster, L. (2009) *Tutorial on Modelling of Gas Turbine Driven Centrifugal Compressors*, PSIG 09A4

Linden, van der, R.J.P and Busking (2013), T.E, Real-Time Optimization of a maturing North Sea Gas Asset with Production Constraints, SPE 167424.

Veeken, K. et al (2010), Gas well liquid loading field data analysis and multiphase flow modelling, Production & Operations, SPE 123657.

